Monte Carlo Studies of Dendrimers. Additional Results for the Diamond Lattice Model

Marc L. Mansfield†

Michigan Molecular Institute, Midland, Michigan 48640

Received October 20, 1998; Revised Manuscript Received August 2, 2000

ABSTRACT: Additional results have been determined for a previously developed model of dendrimers constructed on the diamond lattice. Accurate results are presented through $G = 8$ generations, and some suggestive results at $G = 9$ and $G = 11$ are also reported. The hydrodynamic radius and intrinsic viscosity have been computed according to a Monte Carlo technique that exploits analogies between transport physics and the physics of random walks. Accurate radial density profiles, pair correlation functions, and particle scattering functions are also reported. Ratios of the hydrodynamic and gyration radii change from values expected for linear chains at small G to values expected for spheres at large G. The intrinsic viscosity passes through a maximum at $G = 6$. Radial density profiles indicate extensive back-folding in this model, with end groups dispersed throughout the molecule. The particle scattering functions are in good qualitative agreement with neutron scattering experiments.

1. Introduction

A diamond lattice model of dendrimers has been introduced in previous publications.[1−3] Due to advances in computer power and the development of new computational techniques, it is now possible to report additional and more accurate properties of the model calculated to higher generation numbers. Accurate results are presented here through $G = 9$ generations, and some data are also presented for $G = 11$. The dendrimer model has a ternary core and binary branches, and each spacer is comprised of seven steps on the lattice. Excluded-volume interactions are enforced by forbidding multiple occupancy of any lattice site. The reader should consult earlier publications[1−3] for a complete description of the model.

There have been a few efforts to estimate transport properties of dendrimers.[4−8] Some of these[5,6] follow in the tradition of the Rouse−Zimm model, treating the dendrimer as a θ-state system. These calculations are therefore only valid in the limit of long spacers, for which the dendrimer is relatively dilute and the notion of the θ-state makes sense. Most dendrimers currently being synthesized have relatively short spacers, large internal densities, and very strong excluded-volume interactions. For such systems, these θ-state models are not expected to be valid. In such cases, other sorts of calculations[4,7,8] have been attempted, but these tend to be fairly elaborate and time-consuming. A more powerful technique[9−14] is now available for the estimation of both the translational diffusion coefficient and the intrinsic viscosity, and results are reported here.

An area of controversy in dendrimer science concerns the distribution of the end groups of the molecule. The dominant viewpoint seems to be that the end groups sit predominantly on the outside of the molecule.[15,16] This viewpoint is supported by a certain body of neutron and X-ray scattering data,[17−20] but some NMR experiments[21,22] provide evidence for end groups near the core. Most computer or theoretical models, including this one, display a distribution of end groups throughout the molecule.[22−29] Only one model, that of a polyelectrolyte dendrimer in low salt concentrations,[30] predicts a preponderance of end groups on the exterior. (The DeGennes−Hervet model[31] cannot rightly be said to make such a prediction since it assumes a priori that the end groups are on the exterior.) All views might be correct, with the end group distribution depending on a number of factors and differing from one class of dendrimers to another. It is important to understand these factors and rationalize the various conflicting results.

Table 1. Characteristics of the Model Dendrimer and of the Simulation[a]

G	n	ΔP	m
1	8000	0.25	64
2	8000	0.5	148
3	8000	0.75	316
4	8000	1	652
5	8000	2	1324
6	8000	6	2668
7	6000	20	5356
8	2000	100	10732
9	746	300	21484
11	100	100	85996

[a] G = generation number, n = sample size, $\Delta P = 10^6$ Monte Carlo passes between samples, and m = dendrimer mass in units of occupied lattice sites.

Table 1 summarizes the dendrimer ensembles that were generated and sampled. The value n represents the sample size of the ensemble, and ΔP represents the number of Monte Carlo passes performed between successive samples, in units of 10^6 wiggles.[1] These values of ΔP are adequate to guarantee a high degree of statistical independence between successive samples, except at $G = 9$ and $G = 11$.[1] At $G = 9$ the statistics are still fairly good, while at $G = 11$ the correlation between successive samples is very large. Results given here for $G = 11$, therefore, are only intended to suggest general trends.

Results for hydrodynamic radii, intrinsic viscosity, spherical density profiles, pair distribution functions, and single particle scattering factors are reported in the

† Present address: Department of Chemistry and Chemical Biology, Stevens Institute of Technology, Hoboken, NJ 07030.

10.1021/ma981637u CCC: $19.00
Published on Web 09/29/2000

following sections. Length and mass units are defined so that nearest-neighbor sites on the lattice are $\sqrt{3}$ units apart and so that each segment, i.e., the unit occupying one site of the lattice, has unit mass.

2. Transport Properties: Translational Diffusion and Intrinsic Viscosity

Dilute solution transport properties, mainly intrinsic viscosity and translational diffusion, continue to play an important role in macromolecular characterization. Accurate estimation of these properties for any particular model has always been difficult. Fortunately, techniques for the approximation of transport properties have recently been developed on the basis of analogies between transport problems and other problems in mathematical physics.[9−14] The Navier−Stokes equation governing the flow field about a rigid body, under a particular averaging procedure, transforms into Laplace's equation, with boundary conditions appropriate to problems in electrostatics and in random-walk statistics. The transformation from the Navier−Stokes to Laplace's equation occurs because the Oseen tensor, when averaged over all orientations, is proportional to $1/r$, the Green's function of the Laplacian.

The hydrodynamic radius of a macromolecule, R_h, is defined as the radius of the rigid sphere that possesses the same translational diffusion coefficient as the macromolecule:

$$R_h = kT/6\pi\eta D \tag{1}$$

where k, T, η, and D are Boltzmann's constant, absolute temperature, solvent viscosity, and translational diffusion coefficient, respectively. The analogy with electrostatics is such that[9,10]

$$R_h \cong C \tag{2}$$

where C is the capacitance that the body would have if it were a perfect conductor, at least in the "Gaussian" system of units for which capacitance is measured as a length. A comparison with known results for many bodies indicates that eq 2 is often exact (e.g., triaxial ellipsoids) and is generally valid to within about 1%.[9,10]

In a similar manner, the intrinsic viscosity of a body proves to be analogous to its electrical polarizability.[12,14] A slender body calculation[32] based on the Rouse−Zimm model yields

$$[\eta] \cong \pi m^{-1} \mathrm{Tr}(\alpha) \tag{3}$$

where m is the mass of the body and α is the electrical polarizability tensor that the body would have if it were a perfect conductor (expressed in units such that the dipole moment $\mu = \alpha\cdot\mathbf{E}$) and where Tr represents its trace. However, exact and numerical results for a large number of bodies of many different shapes indicate that the prefactor in eq 3 varies from one body to another, although not strongly:[12]

$$[\eta] = (3.3 \pm 0.2)m^{-1} \mathrm{Tr}(\alpha) \tag{4}$$

The $\pm$ 0.2 in eq 4 accounts for the variations among bodies of different shapes. In this paper, we have used eq 3 to estimate $[\eta]$.

The second analogy is with problems in random-walk statistics and arises because the diffusion equation becomes equivalent to Laplace's equation when integrated from $t = 0$ to $t = \infty$. Imagine that the body sits on the interior of a sphere of radius R. Let b be the probability that a random walker found initially at an arbitrary point on the surface of the sphere adsorbs onto the surface of the body at some later time, and let $1 - b$ represent the probability that the walker escapes to infinity without ever encountering the body. The value b varies in inverse proportion to R, and the capacitance is given exactly as[10−13]

$$C = bR \tag{5}$$

for any R. Monte Carlo techniques can be used to sample an ensemble of random walks, obtaining an estimate for the probability b and therefore arriving at estimates of the capacitance and the hydrodynamic radius. The polarizability tensor, and therefore the intrinsic viscosity, can also be estimated by Monte Carlo calculations on random walks. A full report of the viscosity/polarizability technique is in preparation.[14]

Previous applications[10−13] of this Monte Carlo random-walk algorithm employ random walks in the continuum. However, the Navier−Stokes description of the fluid is obviously invalid over very short length scales. Therefore, it seems permissible to employ coarse-grained random walks, and so we use walks on the same lattice on which the dendrimers are constructed. A full report of this lattice technique will be made elsewhere.[14] When tested on bodies for which the capacitance and polarizability are known, errors are comparable to the ratio of the lattice spacing to the size of the body and therefore comparable to the errors already inherent in the hydrodynamic treatment.

There are three known sources of error in these calculations. Errors are generated by the angular averaging procedure which transforms the Navier−Stokes equation into Laplace's equation, but as noted above, this is in error by no more than a few percent for many bodies. Second, by using lattice random walks rather than continuous ones, we fail to rigorously simulate solutions to Laplace's equation, but also as noted above, relative errors are comparable to the ratio of the lattice spacing to the size of the body. Finally, the approach assumes rigid bodies; we have, in fact, evaluated the hydrodynamic properties of an ensemble of rigid dendrimers. However, Zimm has argued that the rigid-body assumption is not a significant source of error.[33,34]

Table 2 displays the results for the ensemble average hydrodynamic radius. Table 2 also displays ratios of R_h/R_g. This ratio increases from values typical of linear polymers (0.79 and 0.86 respectively have been reported for polystyrene and poly(methyl methacrylate) in θ-solvents[35]), at low G, to values expected for solid spheres, $\sqrt{(5/3)} \cong 1.29$, at high G. This trend reflects the gradual densification of the molecule with increasing G or a transition from high to low draining. It is also consistent with an earlier finding[4] that hydrodynamic estimates of dendrimer size are stronger functions of G than the radius of gyration.

The intrinsic viscosity for these model dendrimers is displayed in Figure 1 and Table 2. The intrinsic viscosity passes through a maximum at $G = 6$. Experimental data display similar maxima.[36,37] The maximum occurs because in the lower generations the internal concentration as a function of generation decreases (much as it does in linear polymers as the molecular weight increases), while in the higher generations it increases.

Table 2. Several Transport and Dimensional Properties, Displayed as Functions of G^a

G	R_h	$[\eta]$	R_g	R_h/R_g	$R_{g,end}$	$R_{g,end}/R_g$	$m[\eta]/3\pi R_h^3$
1	6.39	46.4	7.63	0.84	8.64	1.13	1.20
2	9.79	68.5	10.88	0.90	12.44	1.14	1.14
3	13.92	87.4	14.20	0.98	16.05	1.13	1.09
4	18.81	101.6	17.87	1.05	19.86	1.11	1.06
5	24.62	109.7	21.99	1.12	24.00	1.11	1.03
6	31.53	112.8	26.82	1.18	28.80	1.09	1.02
7	39.67	110.9	32.48	1.22	34.39	1.06	1.01
8	49.03	104.2	39.04	1.26	40.88	1.05	1.01
9	59.65	93.5	46.47	1.28	48.28	1.04	1.00

[a] Length units are such that the embedding diamond lattice has edge length $\sqrt{3}$. Mass units are such that the mass of a dendrimer equals the number of lattice sites it occupies.

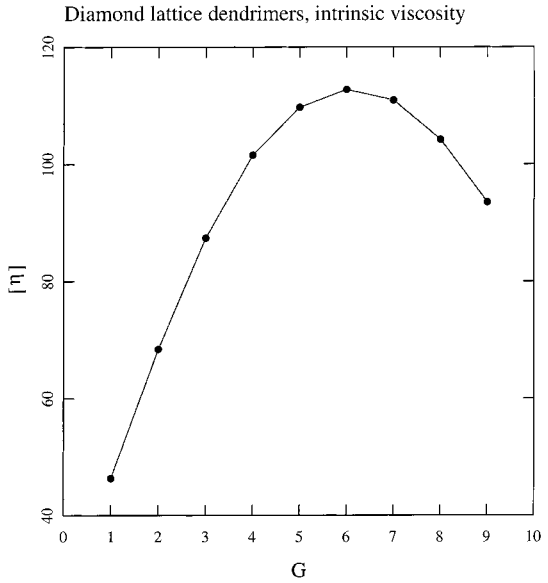

Figure 1. Intrinsic viscosity as a function of G for the model dendrimers.

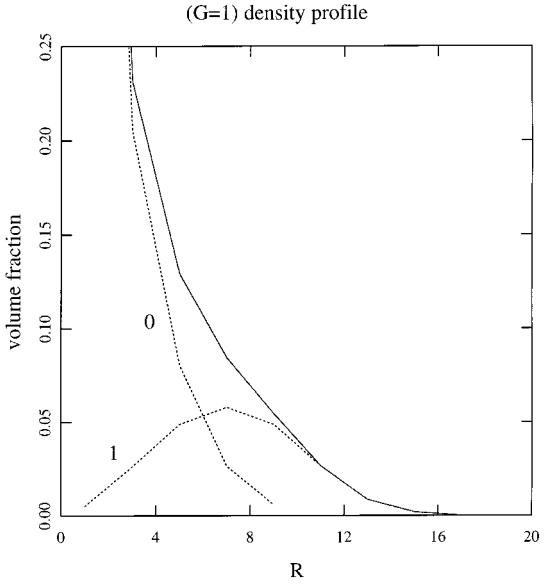

Figure 2. Radial density profile of the $G = 1$ model dendrimer. The solid curve is the density of the entire molecule; dashed curves display the density of each generation.

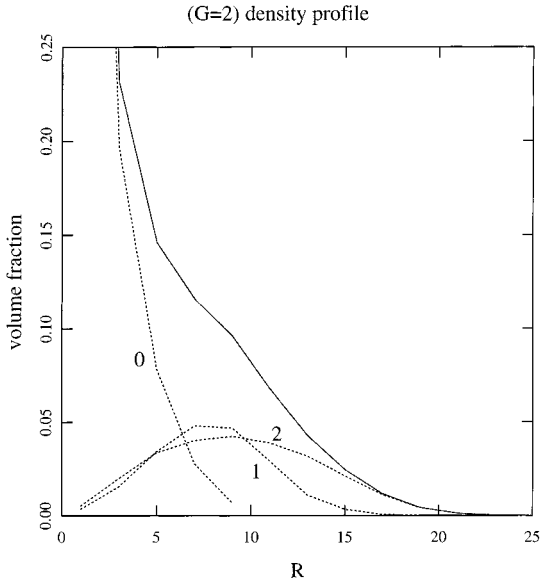

Figure 3. Radial density profile of the $G = 2$ model dendrimer.

Since the capacitance and polarizability of a conducting sphere are R and R^3, respectively,[38] then the ratio $m[\eta]/3\pi R_h^3$ is 1 for a sphere. Table 2 displays this ratio for the model dendrimers. It tends to 1 as G increases, which also indicates a transition from high to low draining.

3. Radial Density Profiles

Figures 2−11 represent the mean radial density of the molecules relative to the core, expressed as a fraction of occupied lattice sites. The curves were obtained at a resolution of 2 length units. Three out of the four lattice sites coordinating the core are of course always occupied, so these curves begin with a peak of height at least 0.75, which extends above the plot. Solid curves represent the complete molecular density, while dashed curves represent contributions from successive tiers.

The behavior shown in these figures follows an interesting trend. For generations 1−3 the density decreases monotonically, and for generations 4−9 a density well appears at $R < 10$ with a maximum at higher R, while for generation 11 the dendrimer density is strikingly uniform. Presumably, the density well in the dendrimers of intermediate generation number arises because the three central spacers bear all the load of the excluded-volume forces between branches and become so highly extended that the remaining parts of the molecule are unable to completely back-fill.[1]

Similar density profiles have been exhibited in a number of related models. For example, the monotonically decreasing densities at $G = 1$, 2, and 3 are also observed in the model studied by Lescanec and Muthukumar.[23] The Lescanec−Muthukumar dendrimers are appropriate models at low G but are inadequate at higher G. (At intermediate and large G, the central spacers are expected to be highly extended. However,

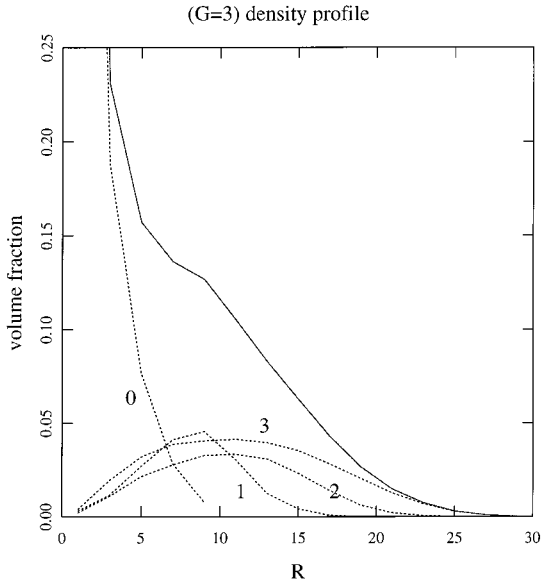

Figure 4. Radial density profile of the $G = 3$ model dendrimer.

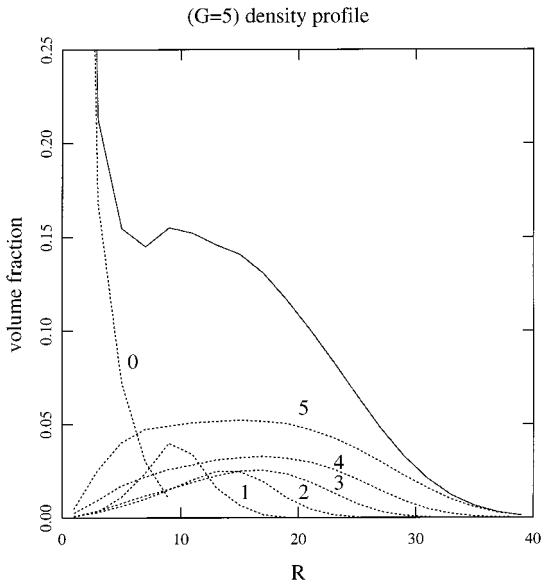

Figure 6. Radial density profile of the $G = 5$ model dendrimer.

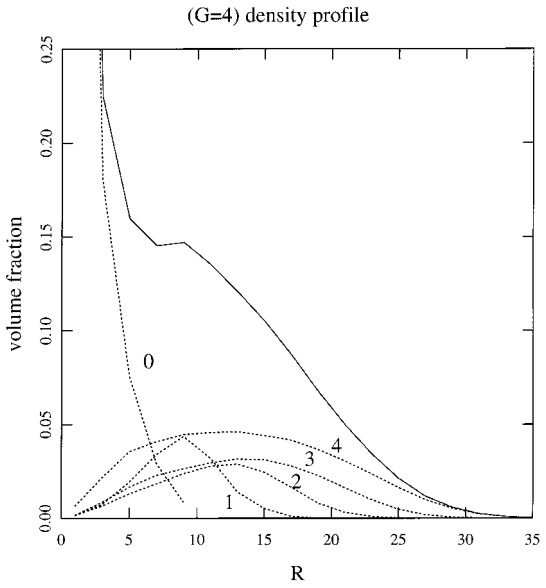

Figure 5. Radial density profile of the $G = 4$ model dendrimer.

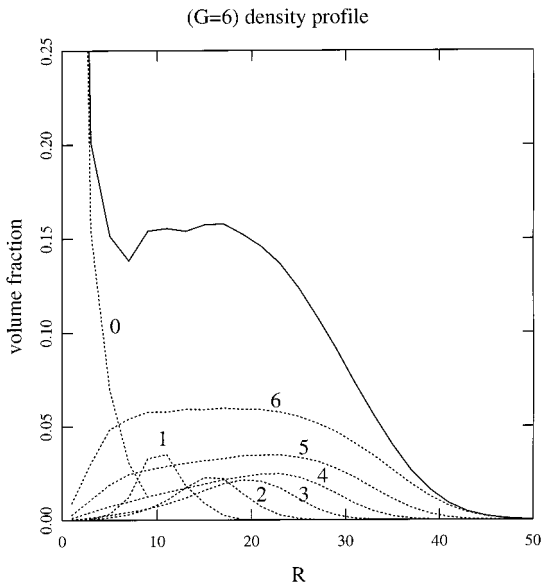

Figure 7. Radial density profile of the $G = 6$ model dendrimer.

since the Lescanec−Muthukumar structures have not been annealed, individual spacers do not depart significantly from ordinary random walks.) Curves such as these, including the density wells in the intermediate generations and the uniform densities in the higher generations, have also been observed in mean-field models.[39]

At every value of G, the terminal generation is observed to be distributed uniformly throughout the molecule. Indeed, at high G, the last few generations are so distributed. Back-folding seems to be a property of all models resembling the present one, i.e., with only short-range repulsions and relatively thin, flexible spacers. On the other hand, a model due to Welch and Muthukumar[30] places most of the end groups on the exterior. This model incorporates a repulsive Debye−Hückel interaction between all pairs of chain ends and is therefore appropriate to polyelectrolytic dendrimers. Under low-salt conditions the Debye−Hückel interaction becomes strong and long-ranged and is able to force the end groups to the exterior. The end groups of dendrimers with bulky, rigid spacers might also lie on the exterior. The role of these factors in determining the end distribution of dendrimers remains unclear.

4. Pair Distribution Functions

Figure 12 displays log−log plots of the pair distribution functions, $g(R)$, of the model dendrimers. For a lattice model such as these, the pair distribution function is the probability that, given a lattice site occupied by some part of the dendrimer, a second lattice site a distance R from the first is also occupied. These curves were prepared with a resolution of 0.25 in R. The complex structure of the curves at low R is of course an artifact of the lattice. In each case, $g(R)$ is near 0.5 for R near $\sqrt{3}$, reflecting the fact that a large majority of segments are attached to exactly two others. Over a range of R from about 6 to about 12−18, depending on G, $g(R)$ can be approximated as a power function: $g(R)$

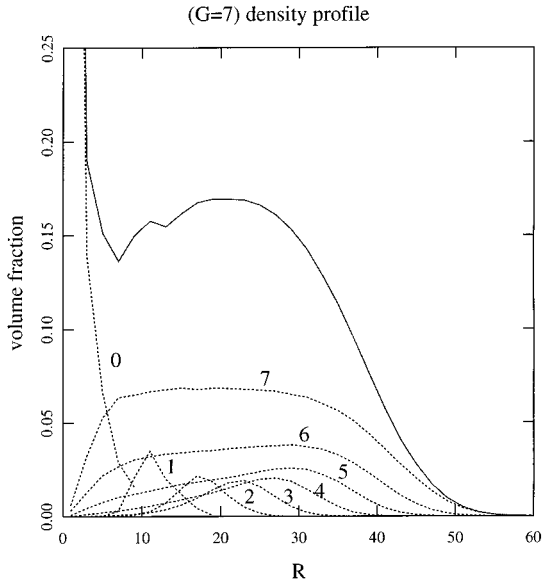

Figure 8. Radial density profile of the $G = 7$ model dendrimer.

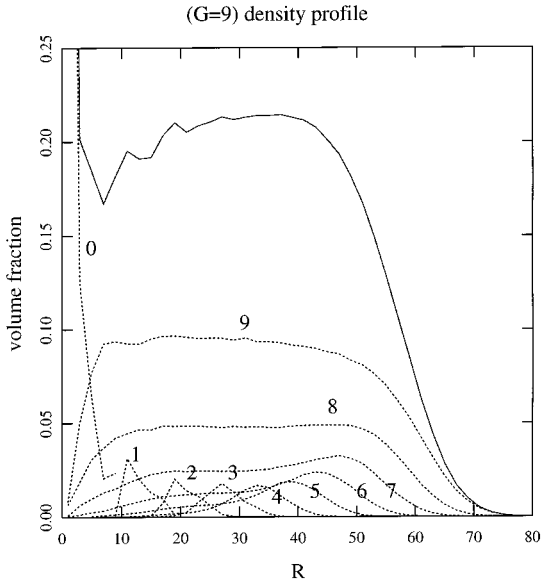

Figure 10. Radial density profile of the $G = 9$ model dendrimer.

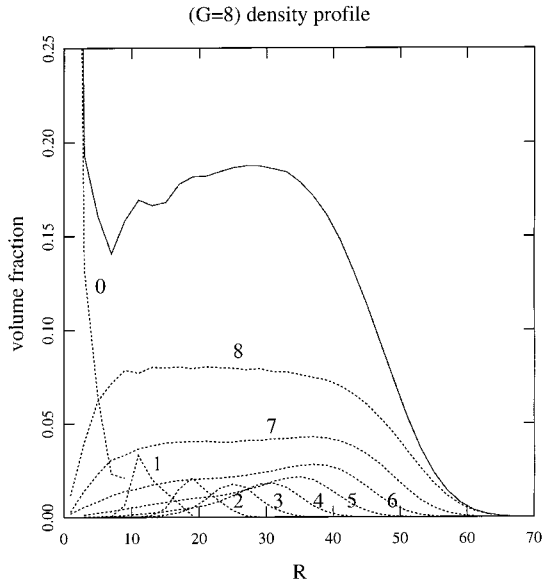

Figure 9. Radial density profile of the $G = 8$ model dendrimer.

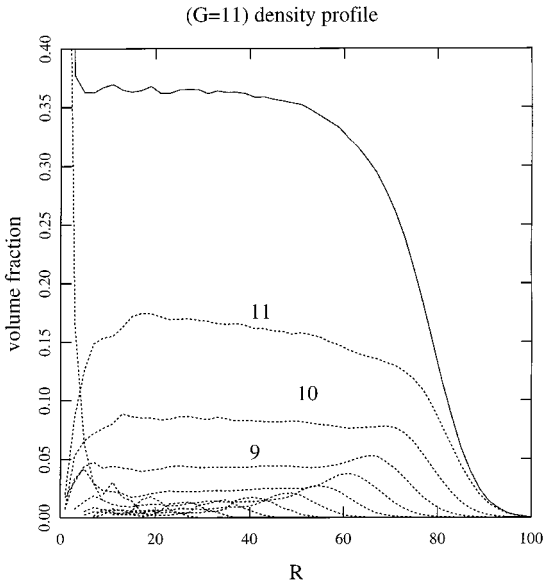

Figure 11. Radial density profile of the $G = 11$ model dendrimer.

$\propto R^{-\lambda}$. Table 3 gives the best-fit values of λ at each value of G.

Power-law behavior of $g(R)$ is commonly taken as evidence that the structure is a fractal. However, $g(R)$ only follows such a law over a limited range of R at best. The dashed lines in Figure 12 represent moderately successful curve fitting rather than any evidence of deep fractal self-similarity. Nevertheless, this behavior suggests that, at least over limited length scales, these model dendrimers fill space in ways comparable to fractals, with inhomogeneous densities and with hierarchical clustering. Therefore, we also present effective fractal dimensions, $F = 3 - \lambda$, in Table 3. F changes with increasing G from values comparable to $^5/_3 \cong 1.7$,[40] which one would expect for a linear chain, to nearly 3, which is expected of space-filling objects. For reasons that are not presently understood, other comparable models are reported to be space filling in all generations; i.e., values of F near 3 are reported.[24]

5. Structure Factors and Gyration Radii

Single-particle structure factors, which can be measured in scattering experiments, are defined as

$$I(q) = N^{-2}\sum_{jk}\langle \exp(i\mathbf{q}\cdot\mathbf{r}_{jk})\rangle \qquad (6)$$

where $\mathbf{q}$ and $\mathbf{r}_{jk}$ represent the wavevector and the displacement between segments j and k, respectively, and where $\langle ... \rangle$ represents an ensemble average, including orientations. The indices j and k run over all scattering centers in the molecule, and N is the number of scattering centers. The behavior of $I(q)$ at small q defines the radius of gyration:

$$R_g^{\,2} = (2N^2)^{-1}\sum_{jk} r_{jk}^{\,2} \qquad (7)$$

Figure 13 displays single-particle structure factors computed for the present model. The structure factors

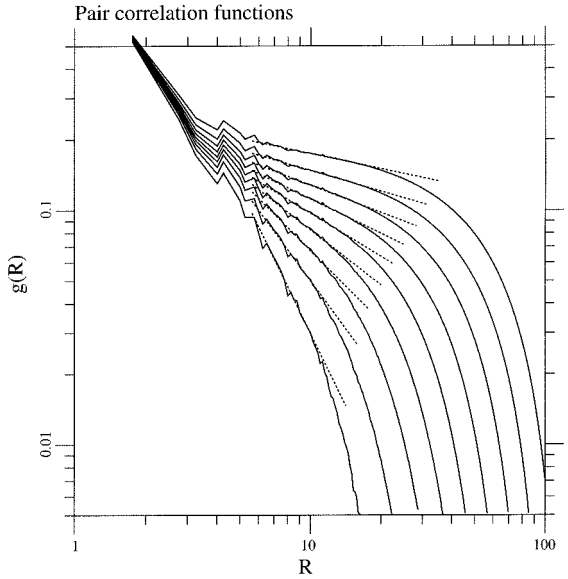

Figure 12. Pair correlation functions of the model dendrimers, progressing from $G = 1$ at the bottom to $G = 9$ at the top. Dashed lines have the slopes given in Table 3.

Table 3. Effective Pair-Distribution Exponents and Fractal Dimensions

G	λ	$F = 3 - \lambda$	G	λ	$F = 3 - \lambda$
1	2.06	0.94	6	0.49	2.51
2	1.36	1.64	7	0.39	2.61
3	1.01	1.99	8	0.29	2.71
4	0.78	2.22	9	0.21	2.79
5	0.61	2.39			

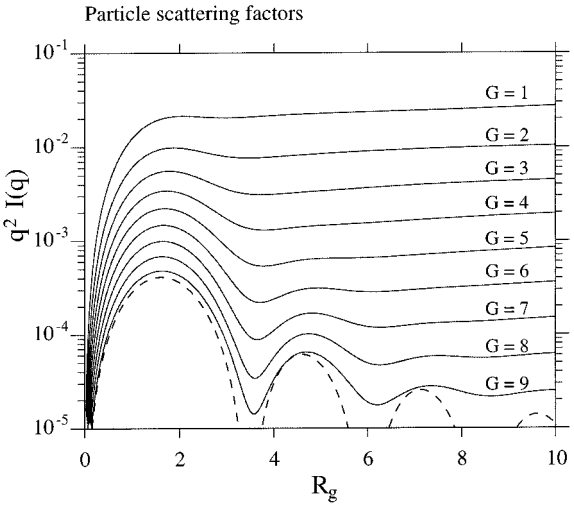

Figure 13. Particle scattering factors of the model dendrimers at all generations through $G = 9$. The dashed curve is the pattern expected for a sphere.

bear a strong qualitative resemblance to the experimental SAXS data of Bauer et al.[17] (For example, see their Figure 1.) Gyration radii are displayed in Table 2.

By selectively labeling the molecule and the solvent, it is possible to probe the internal structure of the molecule. For example, in one experiment, Amis et al.[18] have taken neutron scattering measurements on polyamidoamine dendrimers first with unlabeled dendrimer dissolved in CD_3OH and second with dendrimers bearing deuterium labels only on the last generation and dissolved in a mixed CH_3OH/CD_3OH solvent whose contrast matches that of the unlabeled dendrimer. This is equivalent to letting j and k in eqs 6 and 7 range only over segments in the last generation. Gyration radii for this latter case will be denoted $R_{g,end}$. Values of $R_{g,end}$ computed for the model are displayed in Table 2. For the $G = 7$ model dendrimers, $R_{g,end}/R_g = 1.06$, which is somewhat less than the comparable ratio for the PAMAM dendrimers as measured by Amis et al.,[18] 1.19. In fact, the large value of this ratio is taken by them as evidence that the dendrimer end groups lie on the exterior.

6. Summary and Conclusions

This paper reports new results for a lattice model dendrimer. Using analogies between the physics of transport and of random walks,[9−14] it has been possible to estimate both the hydrodynamic radius and the intrinsic viscosity of the model dendrimers. Ratios R_h/R_g vary from values typical of linear polymers in the low generations to those expected of spheres in the higher generations. The intrinsic viscosity of these dendrimers exhibits a maximum at $G = 6$, in agreement with experiment.

Like many other model dendrimers, the end groups of this model are distributed throughout the molecule. Repulsive polyelectrolyte interactions appear capable of driving the end groups to the surface of the molecule.[30] Other dendrimer properties, for example, spacer bulkiness or flexibility, may also influence the distribution of end groups. The effects of these properties need to be studied systematically.

Over a narrow distance range, pair distribution functions drop off with approximate power law behavior. This indicates that this model fills space like a fractal, with effective fractal dimensions approaching 3 as the generation number increases. However, the range over which this behavior is observed is only about 1 order of magnitude, too small to successfully apply concepts of self-similarity.

Structure factors of the model are in qualitative agreement with the results of X-ray scattering studies.[17] There are discrepancies between the predictions of this model and neutron scattering measurements on end-labeled PAMAM dendrimers.[18] These discrepancies may be due to the fact that the end groups of the PAMAM's are ionic and therefore exhibit the repulsions modeled by Welch and Muthukumar.[30]

Acknowledgment. The author benefited from a number of discussions with Jack Douglas of the National Institutes of Standards and Technology. He also acknowledges the support and encouragement of a number of colleagues at MMI, particularly Donald A. Tomalia and Petar Dvornic. Partial support for this research was provided by the U.S. Army Research Laboratory through the joint ARL/MMI dendrimer program.

References and Notes

(1) Mansfield, M. L.; Klushin, L. I. *Macromolecules* **1993**, *26*, 4262.
(2) Mansfield, M. L. *Polymer* **1994**, *35*, 1827.
(3) Mansfield, M. L. *Polymer* **1996**, *37*, 3835.
(4) Mansfield, M. L.; Klushin, L. I. *J. Phys. Chem.* **1992**, *96*, 3994.
(5) La Ferla, R. *J. Chem. Phys.* **1997**, *106*, 688.
(6) Cai, C.; Chen, Z. Y. *Macromolecules* **1997**, *30*, 5104.
(7) Cai, C.; Chen, Z. Y. *Macromolecules* **1998**, *31*, 6393.
(8) Aerts, J. *Comput. Theor. Polym. Sci.* **1998**, *8*, 49.
(9) Hubbard, J. B.; Douglas, J. F. *Phys. Rev. E* **1993**, *47*, R2983.

(10) Douglas, J. F.; Zhou, H.-X.; Hubbard, J. B. *Phys. Rev. E* **1994**, *49*, 5319.
(11) Zhou, H.-X.; Szabo, A.; Douglas, J. F.; Hubbard, J. B. *J. Chem. Phys.* **1994**, *100*, 3821.
(12) Douglas, J. F.; Garboczi, E. J. *Adv. Chem. Phys.* **1995**, *91*, 85.
(13) Given, J. A.; Hubbard, J. B.; Douglas, J. F. *J. Chem. Phys.* **1997**, *106*, 3761.
(14) Mansfield, M. L.; Douglas, J. F.; Garboczi, E. Manuscript in preparation.
(15) Tomalia, D. A.; Naylor, A. M.; Goddard, W. A., III *Angew. Chem., Int. Ed. Engl.* **1990**, *29*, 138.
(16) Tomalia, D. A. *Adv. Mater.* **1994**, *6*, 529.
(17) Bauer, B. J.; Topp, A.; Prosa, T. J.; Amis, E. J.; Yin, R.; Qin, D.; Tomalia, D. A. *Proc. ACS Div. Polym. Mater. Sci. Eng.* **1997**, *77*, 87.
(18) Amis, E. J.; Topp, A.; Bauer, B. J.; Tomalia, D. A. *Proc. ACS Div. Polym. Mater. Sci. Eng.* **1997**, *77*, 183.
(19) Valachovic, D. E.; Bauer, B. J.; Amis, E. J.; Tomalia, D. A. *Proc. ACS Div. Polym. Mater. Sci. Eng.* **1997**, *77*, 230.
(20) Prosa, T. J.; Bauer, B. J.; Amis, E. J.; Tomalia, D. A.; Scherrenberg, R. J. *J. Polym. Sci., Part B: Polym. Phys.* **1997**, *35*, 2913.
(21) Wooley, K. L.; Klug, C. A.; Tasaki, K.; Schaefer, J. *J. Am. Chem. Soc.* **1997**, *119*, 53.
(22) Gorman, C. B.; Hager, M. W.; Parkhurst, B. L.; Smith, J. C. *Macromolecules* **1998**, *31*, 815.
(23) Lescanec, R. L.; Muthukumar, M. *Macromolecules* **1990**, *23*, 2280.
(24) Murat, M.; Grest, G. S. *Macromolecules* **1996**, *29*, 1278.
(25) Boris, D.; Rubinstein, M. *Macromolecules* **1996**, *29*, 7251.
(26) Chen, Z.-Y.; Cui, S.-M. *Macromolecules* **1996**, *29*, 7963.
(27) Carl, W. *J. Chem. Soc., Faraday Trans.* **1996**, *92*, 4151.
(28) Scherrenberg, R.; Coussens, B.; van Vliet, P.; Edouard, G.; Brackman, J.; de Brabander, E.; Mortensen, K. *Macromolecules* **1998**, *31*, 456.
(29) Keinath, S. E.; Weitz, J., private communication, 1997. A number of molecular models of PAMAM dendrimers were constructed using the Discover package (cvff force field) of Molecular Simulations, Inc. These models all exhibited backfolding following annealing with constant-T molecular dynamics.
(30) Welch, P.; Muthukumar, M. *Macromolecules* **1998**, *31*, 5892.
(31) DeGennes, P.-G.; Hervet, H. J. *J. Phys. (Paris)* **1983**, *44*, L351.
(32) Equation 3 results from a computation of both $[\eta]$ and α for an arbitrary rigid molecule of N beads if Zimm's formalism [ref 33] is used to compute $[\eta]$ and if α is determined by minimizing the total electrostatic energy of the same set of beads in a uniform external field, assuming terms $q_i^2/2a$ for the self-energy of a bead of radius a, and pointlike interactions, q_iq_j/R_{ij}, for the contributions among pairs of beads.
(33) Zimm, B. H. *Macromolecules* **1980**, *13*, 592.
(34) Zimm, B. H. *Macromolecules* **1982**, *15*, 520.
(35) Schmidt, M.; Burchard, W. *Macromolecules* **1981**, *14*, 210.
(36) Tomalia, D. A.; Hedstrand, D. M.; Wilson, L. R. *Encyclopedia of Polymer Science and Engineering*, 2nd ed.; Wiley: New York, 1990.
(37) Mourey, T. H.; Turner, S. R.; Rubinstein, M.; Frechet, J. M. J.; Hawker, C. J.; Wooley, K. L. *Macromolecules* **1992**, *25*, 2401.
(38) Jackson, J. D. *Classical Electrodynamics*, 2nd ed.; Wiley: New York, 1975; p 62.
(39) Mansfield, M. L., unpublished results.
(40) When $G = 1$, F is considerably less than 5/3, but this could very well be due to finite size effects.

MA981637U